ELSEVIER

Journal of Molecular Catalysis A: Chemical 164 (2000) 217–223

JOURNAL OF MOLECULAR CATALYSIS A: CHEMICAL

www.elsevier.com/locate/molcata

Tungstate-modified aluminium phosphate 1. Preparation, characterisation and catalytic activity towards alcohol and cumene conversion reactions

K.M. Parida [a,*], M. Acharya [a], T. Mishra [b]

[a] *Regional Research Laboratory, Bhubaneswar-751 013, Orissa, India*
[b] *NML Field Station, Industrial Estate, Naroda, Ahmedabad-382330, India*

Received 9 January 2000; accepted 6 April 2000

Abstract

A series of tungstate-impregnated aluminium phosphate samples are prepared by varying the tungstate weight percent from 3 to 20 and characterised by XRD and N_2-adsorption–desorption method. Surface areas are found to decrease with increase in tungstate loading. However, tungstate-loaded samples exhibit an increasing trend in acidity and catalytic activity. The sample with 10 wt.% tungstate loading shows highest dehydration and dehydrogenation activity for isopropanol and cumene conversion, respectively. The low C_2^+ hydrocarbon selectivity indicates that the new acid sites formed due to tungstate impregnation is not strong enough to dehydrate methanol to hydrocarbons.

Keywords: Tungstated aluminium phosphate; Alcohol; Cumene

1. Introduction

Amorphous phosphates have found increasing interest as catalyst and catalyst support in the last three decades [1]. Among these phosphates, aluminium phosphate has been studied extensively due to its high surface area, thermal stability and surface acid–base properties [2–7]. To increase its surface acidic properties, the effect of anions like F^-, SO_4^{-2}, etc., have been studied [8]. So, also the effect of transition metal phosphates on the acid base properties of aluminium phosphate is reported [9].

The strong acidity of sulphated metal oxides attracted much attention because of its ability to catalyse a range of reactions such as cracking, alkylation and isomerization [10,11]. As dopant, advantages of tungstate over sulphate include that it does not suffer from dopant loss during thermal treatment and it undergoes significantly less deactivation during catalytic reactions [12]. Tungsten oxide supported on γ-Al_2O_3 or ZrO_2 are the subject of recent investigation due to their high acidity and significant role in important catalytic reactions like selective oxidation, isomerisation and metathesis of olefins [13–17]. Even WO_3 supported $AlPO_4$ is reported as potential hydrotreating catalyst [18]. However, the effect of tungstate on the acid–base properties of $AlPO_4$ is yet to be reported. In this work, we wish to understand the importance of tungstate impregnation towards the acid–base and catalytic properties of aluminium phosphate.

* Corresponding author. Fax: +91-674-581637/581750.
E-mail address: kmparida@yahoo.com (K.M. Parida).

1381-1169/00/$ – see front matter
PII: S1381-1169(00)00249-1

2. Experimental

2.1. Material preparation

Aluminium phosphate was precipitated by adding aqueous ammonia to a solution of $Al(NO_3)_3{\cdot}9H_2O$ and 85% H_3PO_4 with constant stirring till the pH of the solution became 5. The precipitate was filtered, washed with distilled water till free from chloride, dried at 110°C for 12 h and then powdered to −75 to +45 μm.

A series of tungstate-impregnated aluminium phosphate samples were prepared by varying the amount of tungstate loading (3–20 wt.%) by incipient wetness method using ammonium para tungstate. All the samples were dried at 110°C followed by calcination at 500°C for 5 h in air.

2.2. Textural characterisation

The XRD pattern of all the calcined samples were recorded on a Philips semiautomatic X-ray diffractometer using Cu-K_α radiation source and Ni filter in the range of $2\theta = 6^\circ$ to 70°.

The UV–VIS solid state spectra were recorded on Varian UV–VIS spectrophotometer using $BaSO_4$ as reference.

BET surface area, average pore radius, pore size distributions and pore volume were evaluated from N_2 adsorption–desorption isotherm at liquid nitrogen temperature using Quantasorb instrument (Quantachrome, USA). Prior to the adsorption–desorption measurements, all the samples were degassed at 393 K and 10^{-5} Torr for 5 h.

2.3. Catalytic activity

Catalytic activity of all the samples for dehydration/dehydrogenation of 2-propanol and methanol were studied at a steady state condition in a fixed bed catalytic reactor (10 mm, i.d.) with on-line GC. Prior to the reaction, all the catalysts (0.25 g) were heated in nitrogen atmosphere at 400°C for 1 h. Alcohol was supplied to the reactor by bubbling nitrogen gas through the alcohol container at 30°C. To avoid condensation of liquid products in the apparatus, all the connections from the reactor to GC were heated at 120°C by a heating tape. The reaction products were analysed by means of GC (CIC, India) in FID mode using Porapak T and Porapak Q columns.

Cumene cracking/dehydrogenation reaction was carried out in a micropulse reactor (Sigma, India) using nitrogen as carrier gas in the temperature range of 300°C to 500°C. Before the reaction, all the catalysts were activated at 500°C for 1 h in nitrogen stream. The volume of one cumene pulse was maintained at 1 μl (7.2 mmol). All the products were analysed by GC on line with microreactor using 10-ft SS column with 10% TCEP. The conversion level and the product distribution were measured from the average of three pulses.

3. Results and discussion

3.1. Textural and surface properties

The XRD patterns of pure aluminium phosphate along with 3 and 10 wt.% tungstated aluminium phosphate reveal the amorphous pattern of the materials. However, aluminium phosphate containing more than 10 wt.% tungstate are poorly crystalline and the peaks at d=3.77, 3.70, 3.64, 2.64 and 2.62 may be due to the presence of $W_{18}O_{49}$ and/or WO_3 crystalline phases. The broadening of adsorption band around 300 nm in the UV–VIS spectra of sample (Fig. 1) with 10 wt.% tungstate loading also indicate the formation of poly-tungstate species [19].

Surface and textural parameters of all the samples are given in Table 1. The BET surface area of pure

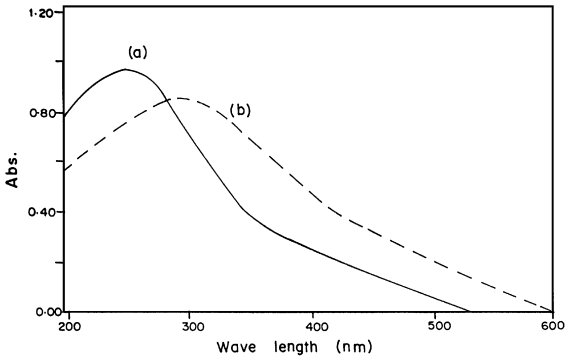

Fig. 1. Diffuse reflectance spectra of tungstated aluminium phosphate. (a) 10 wt.% WO_4^{-2}–$AlPO_4$ and (b) 13.4 wt.% WO_4^{-2}–$AlPO_4$.

Table 1
Surface parameters of tungstated aluminium phosphate calcined at 500°C

Sample code	WO_4^{-2} (wt.%)	S_{BET} (m^2/g)	R_{av} (Å)	S_t (m^2/g)	V_p (cm^3/g)
$AlPO_4$	0	120	30.8	123	0.185
3.0 WO_4^{-2}–$AlPO_4$	3.0	90	40.4	94	0.182
6.7 WO_4^{-2}–$AlPO_4$	6.7	85	42.3	83	0.18
10.0 WO_4^{-2}–$AlPO_4$	10.0	83	41.2	80	0.171
13.4 WO_4^{-2}–$AlPO_4$	13.4	81	41.8	79	0.17
20.0 WO_4^{-2}–$AlPO_4$	20.0	60	39.0	56	0.117

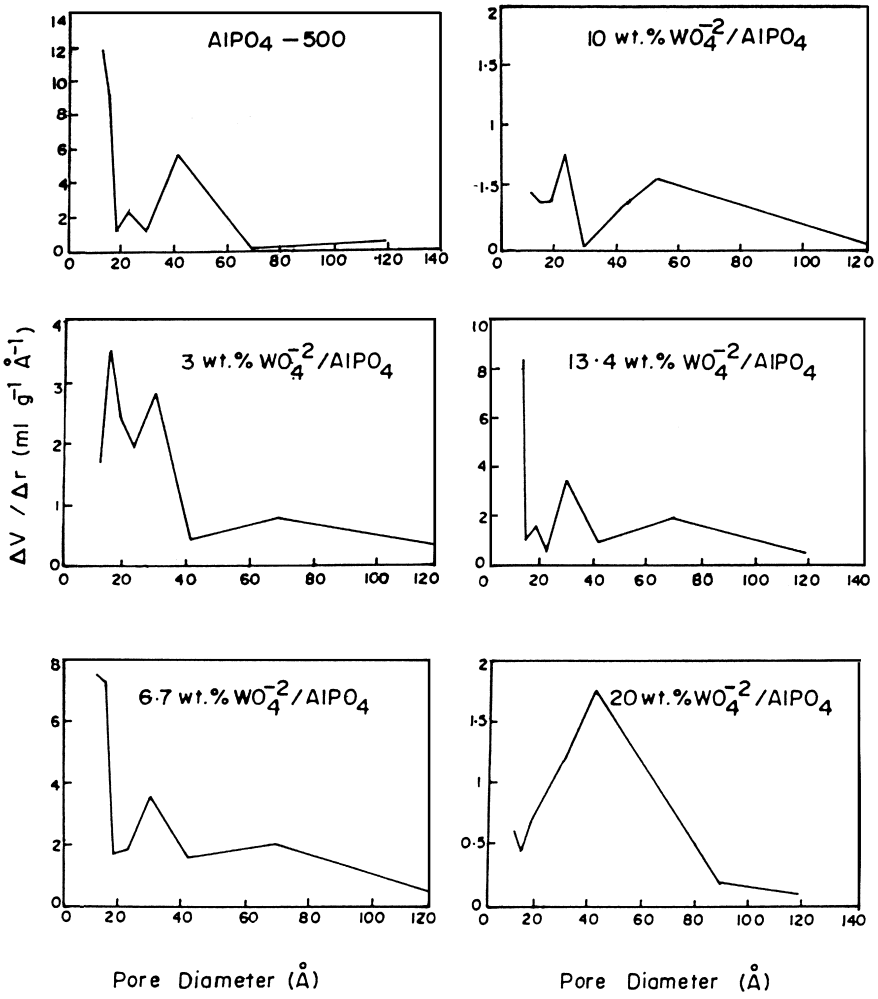

Fig. 2. Distribution of pore sizes as a function of pore diameter.

aluminium phosphate is 120 m^2/g and this along with the pore volume decreases with tungstate loading. This imply no new pores are generated by tungstate treatment rather it blocks the pores, thereby decreasing the surface area. The nitrogen adsorption–desorption isotherm depicts that the materials is mesoporous (Fig. 2). Assuming the pores to be cylindrical, the average pore radius is calculated by using the formula $r=2V_p/S_p$, where r is the average pore radius, V_p is the pore volume and S_p is the specific internal surface area of the pores. The average pore radius calculated by the above method are tabulated in Table 1. It is found that the average pore radius increases due to the tungstate impregnation. However, with the variation in tungstate loading, there is no variation in average pore diameter. The surface area calculated from BET and t-plot methods (S_t) are very similar and the upward deviation in the t-plot also confirm the mesoporosity.

3.2. Catalytic activities

3.2.1. Alcohol conversion

The 2-propanol conversion produces propene as the major and acetone as the minor product in all the samples. In case of tungstate samples, the reaction starts at 150°C while for pure aluminium phosphate, the reaction starts at 200°C. It is observed that the tungstate loading increases the propene formation (Fig. 3) to an appreciable extent. Further, it is found that the acetone selectivity decreases with the increase in tungstate loading up to 10 wt.% and thereafter it remain same. The increment in propene formation of these samples may be correlated to the increase in the number of acid sites due to the presence of tungstate on $AlPO_4$. However, it has been found that in case of all the tungstate-impregnated aluminium phosphate, i.e. 3 to 20 wt.%, there is an increase in propene formation up to 10 wt.% of the tungstate sample and thereafter it decreases. So, the 20-wt.% loaded sample shows nearly the same catalytic activity as that of pure $AlPO_4$. This decrease may be due to the formation of di- or poly-tungstate at higher tungstate loading on the surface of aluminium phosphate which is already evidenced from XRD and UV–VIS spectra.

Generally, alcohols dehydrate on acid sites to give ether and olefins. Again, the selectivity to a particular product is determined by alcohol structure (primary, secondary), reaction temperature, and surface acidity of the catalyst. As the basicity of 2-propanol is higher than the primary alcohols, it can give olefin as the major product even on weak acid sites, whereas methanol dehydrates to olefins only on strong acid sites. Therefore, to differentiate between the strong and weak acid sites, methanol conversion was carried out on all the samples. The observed trend of methanol conversion (Fig. 4) is the same as in case of 2-propanol. Pure $AlPO_4$ gives DME as major product at all reaction temperature having C_2+ hydrocarbon selectivity within 2% only at higher reaction temper-

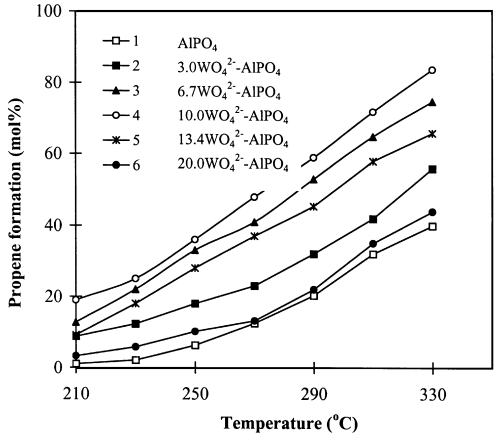

Fig. 3. Propene formation on tungstated aluminium phosphate calcined at 500°C.

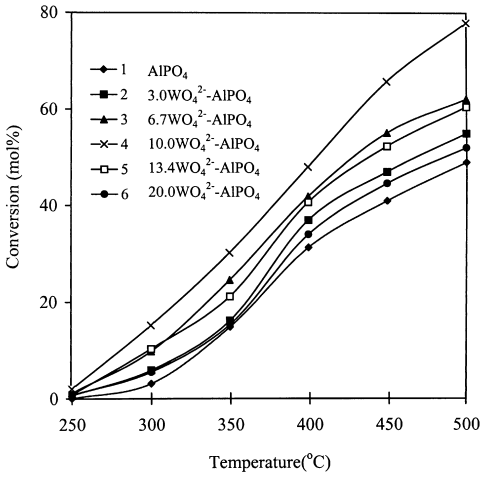

Fig. 4. Methanol conversion on tungstated aluminium phosphate calcined at 500°C.

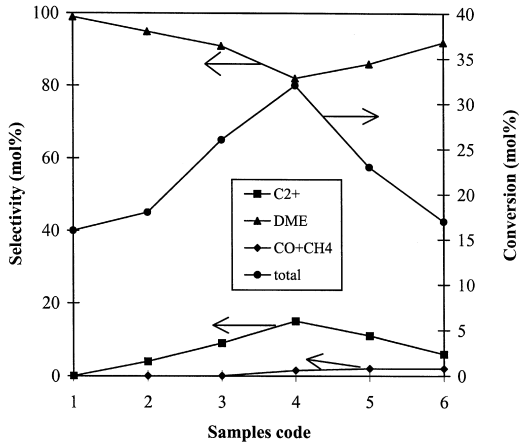

Fig. 5. Product selectivity for methanol conversion over different catalysts at 350°C. Here, 1,2,3,..., 6 represent $AlPO_4$, 3.0 wt.% WO_4^{-2}–$AlPO_4$, 6.7 wt.% WO_4^{-2}–$AlPO_4$, 10.0 wt.% WO_4^{-2}–$AlPO_4$, 13.4 wt.% WO_4^{-2}–$AlPO_4$, 20 wt.% WO_4^{-2}–$AlPO_4$, respectively.

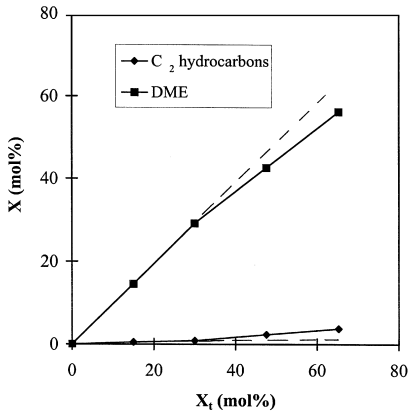

Fig. 6. OPE plot for methanol conversion on 10 wt.% WO_4^{-2}–$AlPO_4$ at 325°C.

ature. However, with tungstate loading, not only the total conversion but also C_2+ hydrocarbon selectivity increases (Fig. 5) and the highest selectivity is observed in case of 10 wt.% loaded catalyst. Decomposition product of DME is not observed over pure $AlPO_4$ but with tungstate-loaded samples it is noticed in low amount (2 mol%). From both the alcohol conversion data, it is observed that the sample with 10 wt.% tungstate loading exhibit highest dehydration activity among all the prepared samples. Comparatively, low C_2+ hydrocarbon selectivity ($\geq$15 mol%) indicates that the new acid sites formed due to tungstate impregnation are not strong enough to dehydrate methanol to hydrocarbons. The low propene and C_2+ hydrocarbon conversion selectivity over the samples having more than 10 wt.% tungstate suggest that the excess amount of tungstate creates the hindrance to the existence of acid sites due to the accumulation on the surface of the catalyst. Thus, the surface area, pore volume and product selectivity decreases.

Selectivity of the products in the reaction are represented by their corresponding optimum performance envelop (OPE) curves. These are obtained by plotting the fractional conversion (X) of a particular product against the total conversion (X_t). This is obtained by varying catalyst to alcohol ratio (w/w) as described by Ko and Wojcieehowki [20]. The OPE curves represent the conversion selectivity behaviour of active sites present on a catalyst and whose slope at the origin represents the initial selectivity for those products. For obtaining the product distribution as a function of the conversion, we have included experiments performed by varying the weight of the catalyst, so that conversion as high as 40–50 mol% can be achieved. The OPE plot of 10 wt.% tungstated aluminium phosphate (Fig. 6) gives two straight lines owing to the formation of DME and C_2+ hydrocarbons. At certain point, it is noticed that the DME plot moves downward while the C_2+ hydrocarbon line moves upwards. This indicates that DME gives C_2+ hydrocarbons on further dehydration on a secondary reaction over tungstated $AlPO_4$ samples. So, C_2+ hydrocarbons is a primary and secondary product.

3.2.2. Cumene cracking/dehydrogenation

Cumene on acidic catalysts gives cracking and dehydrogenation products. Cracking produces benzene and propene as the products while α-methyl styrene is the dehydrogenation product. Over pure $AlPO_4$, only α-methylstyrene is found as the product at all reaction temperatures (Table 2). However, with increase in tungstate loading, total conversion as well as benzene selectivity increases. From the benzene and α-methylstyrene ratio, it is well marked that the α-methylstyrene selectivity is more in all cases. Inability of the pure $AlPO_4$ towards the cracking products indicates the absence of Brönsted acid sites or Lewis basic sites [21]. With tungstate impregnation,

Table 2
Cumene conversion over tungstate-promoted $AlPO_4$ at different temperatures[a]

Reaction temperature (°C)	Total conversion (mol%)					
	1	2	3	4	5	6
300	3(0.0)	5(0.25)	6(0.33)	8(0.33)	8(0.28)	5(0.25)
350	5(0.0)	9(0.29)	10(0.43)	14(0.40)	12(0.41)	10(0.40)
400	8(0.0)	15(0.36)	17(0.54)	21(0.55)	20(0.48)	17(0.44)
450	13(0.0)	21(0.40)	24(0.60)	30(0.66)	28(0.55)	23(0.53)
500	19(0.0)	30(0.66)	33(0.82)	40(0.95)	36(0.80)	32(0.68)

[a] Figures in the parenthesis are the ratio of benzene to α-methyl-styrene in the product. Here, 1,2,3,..., 6 also represent $AlPO_4$, 3.0 WO_4^{-2}–$AlPO_4$, 6.7 WO_4^{-2}–$AlPO_4$,..., 20.0 WO_4^{-2}–$AlPO_4$, respectively.

new acid sites are formed, thereby increasing the total conversion as well as cracking activity. It is believed that cracking reaction proceeds over Brönsted acid sites while dehydrogenation proceeds over Lewis acid sites. Therefore, it can be assumed that the new acid sites are both Brönsted and Lewis types. However, the high selectivity of dehydrogenation product suggests the presence of higher number of Lewis acid sites.

Further, it was observed that with the increase in tungstate content, both the cracking and dehydrogenation product increases up to 10 wt.% loading. But thereafter, it suddenly falls. This decrease in cumene conversion at higher tungstate loading may be due to segregation of tungstate group over the matrix surface, thus lowering the number of available acid sites. However, in the OPE plot of 10 wt.% tungstated aluminium phosphate (Fig. 7), both the product lines (corresponding to benzene and α-methyl styrene) are straight without any deviation, indicating the formation of the two primary stable products.

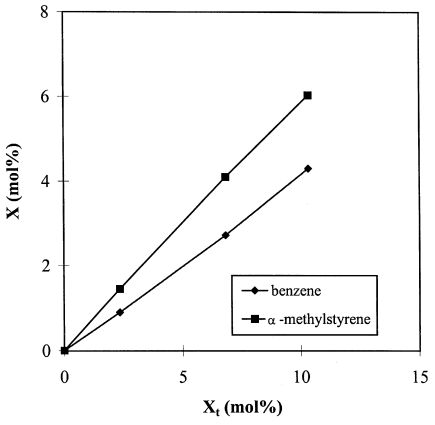

Fig. 7. OPE plot for cumene conversion over 10 wt.% WO_4^{-2}–$AlPO_4$ at 350°C.

3.2.3. Poisoning studies

The Poisoning of active sites of tungstate-loaded $AlPO_4$ catalysts in the 2-propanol and cumene conversion reactions were performed by presaturation of the acid sites with pyridine (PY) and 2,6-dimethyl pyridine (DMPY). The catalysts were saturated with the probe molecules in the nitrogen stream. The catalyst bed was flushed with nitrogen at 573 K for 45 min to remove the unreacted base from the catalyst surface [22–24]. In this way, PY was bonded to both Brönsted and Lewis acid sites [22,23], whereas DMPY is only bonded to the Brönsted acid sites [22–24].

Propene conversion decreases up to 50% on PY adsorbed catalyst in comparison to the same catalyst before PY adsorption, while the decrease is about 70% on DMPY adsorbed samples. As DMPY preferentially adsorbed on Brönsted acid sites, the decrease in dehydration activity shows that the 2-propanol dehydration mainly occurs on Brönsted acid sites, thus strengthening the carbenium ion mechanism.

At the same time, cumene cracking activity of all the samples becomes nearly zero due to DMPY adsorption. However, dehydrogenation activities remain the same for DMPY adsorption, while it decreases to 65% due to PY adsorption. Therefore, it can be concluded that mostly Brönsted acid sites are responsible for cracking and Lewis acid sites are equally responsible for dehydrogenation activity. So, it is understood from the product selectivity that the tungstate-loaded

$AlPO_4$ contain mainly Lewis acid sites. In contrary to this, most of the acid sites due to tungstate impregnation on ZrO_2 is of Brönsted type [25].

4. Conclusions

The above study reveals that the surface acidity of pure aluminium phosphate increased with tungstate impregnation up to 10 wt.% and thereafter decreases with increase in loading. From the catalytic reactions and activity studies, it is understood that the increase in surface acid sites is due to the formation of Lewis acid sites. However, the catalytic activity decreases suddenly after 10 wt.% of tungstate loading. This decrease may be due to polymerization of tungstate species. However, the supported tungstate catalysts show higher activity than the conventional pure aluminium phosphate catalyst. Although tungstate impregnation increases the acid strength of pure $AlPO_4$, this material is not as acidic as tungstated ZrO_2.

Acknowledgements

The authors are thankful to Prof. H.S. Ray, Director, Regional Research Laboratory, Bhubaneswar, and Prof. P. Ramachandra Rao, Director, NML, Jamshedpur, for their permission to publish this paper and Dr. S.B. Rao, Head, IC Division, for his constant encouragement throughout this work.

References

[1] J.B. Moffat, Catal. Rev. Sci. Eng. 18 (1978) 199.
[2] Y. Sakai, H. Hattori, J. Catal. 42 (1976) 37.
[3] R.F. Vogel, G. Marcelin, J. Catal. 80 (1983) 492.
[4] A. Schmideyer, J.B. Moffat, J. Catal. 96 (1985) 242.
[5] H. Jtoh, A. Tada, H. Hattori, K. Tanabe, J. Catal. 115 (1989) 244.
[6] B. Rebenstorf, T. Lindblad, S.L.T. Anderson, J. Catal. 128 (1991) 293.
[7] G.J. Hutchings, I.D. Hudson, D. Bethell, D.G. Timms, J. Catal. 188 (1999) 291.
[8] J.M. Campelo, A. Gorcia, J.M. Gutiemez, D. Zuma, J.M. Marinas, J. Colloid Interface Sci. 95 (1983) 544.
[9] T. Mishra, K.M. Parida, S.B. Rao, Appl. Catal., A 166 (1998) 115.
[10] K. Arata, Adv. Catal. 37 (1990) 165.
[11] D.A. Ward, E.I. Ko, J. Catal. 150 (1994) 15.
[12] G. Larsen, E. Lotero, R.d. Rawa, Proc. 11th Int. Congr. Catal. (1996) 543.
[13] M. Hino, K. Arata, J. Chem. Soc., Chem. Commun. (1987) 1259.
[14] S.L. Soled, E. Gates, E. Ighesia, U.S. Patent 5,422,327, 1995.
[15] S. Meijers, L.H. Gielgans, V. Ponce, J. Catal. 156 (1995) 147.
[16] J. Engweiler, J. Harf, A. Baiker, J. Catal. 159 (1996) 259.
[17] D.s. Kim, M. Ostromecki, I.E. Wachi, Catal. Lett. 33 (1995) 209.
[18] L.J. Lakshmi, P.K. Rao, V.M. Mastikhin, A.V. Nason, J. Phys. Chem. 97 (1993) 11373.
[19] L.G. Gielgens, M.G.H. Vanksmpen, M.M. Broek, R. Vanltardeveld, V. Ponee, J. Catal. 154 (1995) 201.
[20] A.N. Ko, B.W. Wojcieehowki, Prog. React. Kinet. 12 (1983) 201.
[21] G. Wendt, Z. Chem. 17 (1977) 118.
[22] H.A. Benesi, J. Catal. 28 (1973) 176.
[23] A. Corma, C. Rodellas, V. Fornes, J. Catal. 88 (1984) 324.
[24] L.L. Murrell, N.C. Dispenzieve, J. Catal. 117 (1989) 275.
[25] R.A. Boyse, E.I. Ko, J. Catal. 171 (1997) 191.